

## Cytotoxic turrianes of *Kermadecia elliptica* from the New Caledonian rainforest

Claire Jolly<sup>a</sup>, Odile Thoison<sup>a</sup>, Marie-Thérèse Martin<sup>a</sup>, Vincent Dumontet<sup>a</sup>, Aline Gilbert<sup>a</sup>,  
Bruno Pfeiffer<sup>b</sup>, Stéphane Léonce<sup>b</sup>, Thierry Sévenet<sup>a</sup>,  
Françoise Guéritte<sup>a</sup>, Marc Litaudon<sup>a,\*</sup>

<sup>a</sup> Institut de Chimie des Substances Naturelles, CNRS, 1, Avenue de la Terrasse, 91198 Gif-sur-Yvette Cedex, France

<sup>b</sup> Institut de Recherche Servier, 125 Chemin de Ronde, 78290 Croissy-sur-Seine, France

Received 28 May 2007; received in revised form 3 July 2007

Available online 7 September 2007

### Abstract

In the course of an automated screening for small molecules presenting cytotoxic activity, eight new cyclophanes named kermadecins A–H (**1–8**), have been isolated from the bark of a New Caledonian plant, *Kermadecia elliptica*, Proteaceae. A LC/APCI-MS study performed on kermadecins A, B and C, provided a reliable method for the detection of other analogues existing in small quantities in the extract. This led to the isolation of five other members of this chemical series. The structures were elucidated by extensive mono- and bi-dimensional spectroscopy and mass spectrometry. The cytotoxic activity of four of them was evaluated on various cell lines.

© 2007 Published by Elsevier Ltd.

**Keywords:** *Kermadecia elliptica*; Proteaceae; Kermadecin; Turriane; Cyclophane; Cytotoxicity; LC/APCI-MS

### 1. Introduction

With the objective to discover new bioactive compounds from the New Caledonian flora, *Kermadecia elliptica* Brongniart & Gris, (Proteaceae) was selected for a phytochemical study following its potent cytotoxicity against KB cells. The EtOAc extract of the bark exhibited 100% and 44% inhibition of the cell growth at 10 and 1  $\mu\text{g ml}^{-1}$ , respectively. Bioassay and LC/MS-directed fractionations of the EtOAc extract provided eight new cyclophanes, named kermadecins A–H (**1–8**). These compounds are derivatives of the (14-*p*,0-*o*)cyclophane skeleton (**9**) and belong to the turriane family. Turrianes were isolated first from two Australian Proteaceae, *Grevillea striata* (Ridley et al., 1970) and *G. robusta* (Cannon et al., 1973; Chuang

and Wu, 2007). Those turrianes were shown to be potent DNA cleaving agents under oxidative conditions when evaluated in the presence of copper ion and butylamine (Furstner et al., 2002). The skeleton of kermadecin D (**4**) was also found in grevirobstol B isolated from *Grevillea robusta* (Ahmed et al., 2000). A literature survey revealed that the *Kermadecia* species had never been studied for their secondary metabolite content.

The Proteaceae are an archaic family of tropical plants that are mostly represented in Africa and Australia. There are more than 1300 species all over the world. The genus *Kermadecia* is well represented in New Caledonia with 4 endemic species. No report is mentioned regarding their utilisation by traditional healers. Naphthoquinones (Mock et al., 1973), tropane alkaloids (Bick et al., 1979; Butler et al., 2000; Lounasmaa et al., 1980), phenols (Cannon and Metcalf, 1971) and  $\beta$ -sitosterol (Ritchie et al., 1965) have been isolated from other Proteaceae. The structures of compounds **1** to **8** were identified by NMR spectroscopic

\* Corresponding author. Tel.: +33 1 69 82 30 85; fax: +33 1 69 07 72 47.  
E-mail address: [litaudon@icsn.cnrs-gif.fr](mailto:litaudon@icsn.cnrs-gif.fr) (M. Litaudon).

and mass spectroscopic analysis. Four of the eight new turrianes were submitted to cytotoxicity assays. Two of them (**1–2**) showed significant cytotoxicity against KB and L1210 cancer cell lines.

## 2. Results and discussion

*Kermadecia elliptica* was collected in the rain forest “Forêt Plate” in the west central chain of New Caledonia, known as “Grande Terre”. The air-dried bark was extracted successively with EtOAc and MeOH. The EtOAc extract was found to be the most cytotoxic, producing 100% and 44% of inhibition of the KB cell growth at 10 and 1  $\mu\text{g ml}^{-1}$ , respectively. Bioassay-guided fractionation of the active fraction led to the isolation of three new compounds: kermadecins A–C (**1–3**). A LC/MS method was then used to detect and to direct further purifications leading to the isolation of kermadecins D–H (**4–8**). Based on NMR data obtained from  $^1\text{H}$ ,  $^{13}\text{C}$ , COSY, HSQC and HMBC experiments, the compounds could be identified as turrianes (Fig. 1).

A preliminary LC/APCI-MS study of kermadecins A (**1**), B (**2**) and C (**3**) revealed to be particularly efficient due to the low polarity of this kind of compounds and the presence of phenols which gave reliable ionisations in both positive- and negative-ion modes. The LC/MS-MS study was then performed on all the fractions with the aim to find minor compounds of the same family. This led to the isolation of kermadecins D–H (**4–8**). The presence of common fragments was systematically observed in MS-MS. In negative-ion mode, LC/MS-MS analyses of the quasimolecular peak  $[\text{M}-\text{H}]^-$  of kermadecins A and B (**1** and **2**) showed the presence of an ion at  $m/z = 369$  corresponding to the loss of a fragment of 108 amu, suggesting the loss of the dimethylpyran ring as shown in Fig. 2. The presence of this ion was also observed

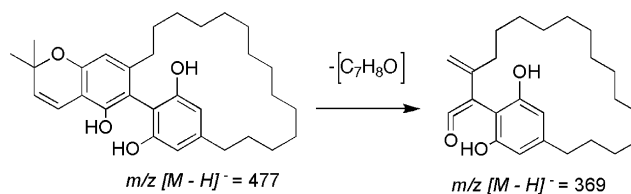


Fig. 2. Hypothesis of fragmentation of kermadecin A in APCI negative-ion mode.

in the mass spectrum of kermadecins D, E, and G (**4**, **5**, **7**). It is interesting to note that an ion at  $m/z$  107 is also systematically observed in the MS spectra for compounds **1**, **2**, **4** and **6** having the dimethylpyran fused to the phenol moiety. In the case of kermadecin E (**5**), a fragment of 110 amu was lost, corresponding to the open heterocycle; this time an ion at  $m/z$  109 was observed. Finally, it is worthy to note that the fragmentation did not occur for kermadecin C (**3**), which possesses a paraquinone moiety fused to the heterocycle. In APCI positive-ion mode, LC/MS-MS analysis of kermadecins A–C (**1–3**) indicated the presence of another ion at  $m/z = 297$ , resulting of the loss of a 182 amu fragment, which was supposed to be a 14 carbons long chain. This fragmentation, which could correspond to two kinds of ions (Fig. 3), was systematically observed for all the compounds of the series, indicating that they all have a 14 carbon aliphatic chain. In the case of kermadecin H (**8**), a fragment of 180 amu was lost, suggesting the presence of a double bond in the aliphatic chain.

Compound **1** has a molecular formula  $\text{C}_{31}\text{H}_{42}\text{O}_4$  supported by HRESIMS showing a  $[\text{M} + \text{Na}]^+$  ion peak at 501.3071 (calcd. 501.2981). The IR spectrum of **1** showed absorption bands at  $3518\text{ cm}^{-1}$  for hydroxy groups and at  $1616$  and  $1426\text{ cm}^{-1}$  for an aromatic ring suggesting that compound **1** was a phenolic compound. The UV absorption  $\lambda_{\text{max}}$  (MeOH) at 280 nm ( $\log \epsilon$  4.15) was indicative

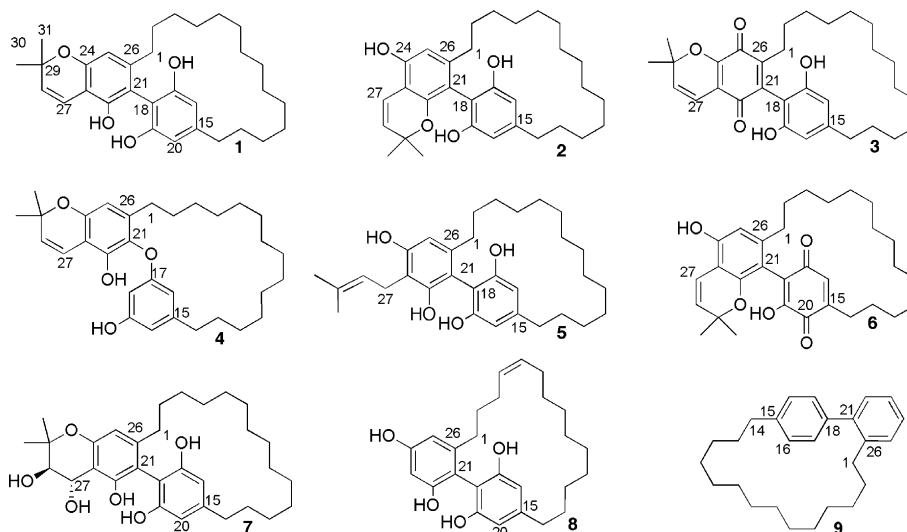


Fig. 1. Structures of kermadecins A–H (**1–8**) and (14-*p,o*)cyclophane skeleton (**9**).

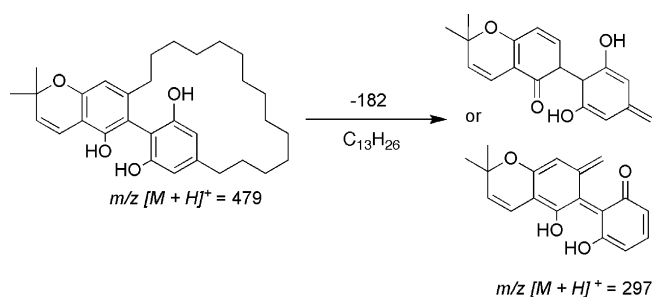


Fig. 3. Hypothesis of fragmentation of kermadecin A in APCI positive-ion mode.

of a bis-benzyl group. The  $^1H$  NMR and  $^{13}C$  NMR (Tables 1 and 2) spectra of compound **1** confirmed the presence of aromatic rings, a long carbon chain, two vinylic protons and two equivalent methyl groups. In the aromatic part of the  $^1H$  NMR spectrum, three aromatic protons appearing as one proton singlet at  $\delta$  6.44 (1H, *s*) and two-protons singlet at  $\delta$  6.45 (2H, *s*) suggested the presence of a penta-substituted and a symmetrical tetrasubstituted aromatic rings, respectively. This was also confirmed in the  $^{13}C$  NMR spectrum by the presence of nine quaternary aromatic carbons (four oxygenated) and three aromatic methines. Moreover the  $^1H$  NMR spectrum showed also signals assignable to a 2,2-dimethylpyran ring. Finally, two olefinic carbon signals and seventeen aliphatic carbon signals due to fourteen methylenes, two equivalent methyls and one quaternary (oxygenated) carbon, were observed in

the  $^{13}C$  NMR and DEPT spectra. In the HMBC experiment, correlations observed between H-27 ( $\delta$  6.62, *d*,  $J_{6,7} = 10$  Hz) and carbons C-22 ( $\delta$  150.7), C-23 ( $\delta$  107.5), C-24 ( $\delta$  155.3) and C-29 ( $\delta$  76.6) suggested that the dimethylpyran ring is fused to the first aromatic ring. Long-range correlations from H-25 to C-1, H-1 to C-21 and C-25 and H-20 to C-14 in the HMBC spectrum confirmed the location of a long carbon chain attached between the two aromatic rings (Fig. 4). The absence of any other C–H correlations between methylene groups and aromatic carbons suggested that the two aromatic rings are directly bound as depicted in **1**. In contrast to compound **2**, no NOE interaction between the aromatic singlet H-25 ( $\delta$  6.44, *s*) and the hydroxy proton singlet at  $\delta_H$  4.98 was observed, indicating that the dimethylpyran ring was located as shown in **1**. These data, together with other results from COSY and HMBC analysis, shown by arrows in Fig. 5, confirmed the structure of kermadecin A **1**.

The HRESIMS of **2** indicated a molecular formula of  $C_{31}H_{42}O_4$  deduced from the ion peak at  $m/z$  501.3072  $[M + Na]^+$  (calcd. 501.2981). Most NMR signals of compound **2** were nearly similar to that of **1** suggesting the presence of the same aromatic rings as in **1**, one dimethylpyran ring fused to one aromatic ring and a long carbon chain attached to both aromatic rings. NOESY experiment, obtained in DMF at a temperature of 233 K was useful to determine the location of the dimethylpyran ring (Fig. 5). Cross peak was indeed observed between H-25 ( $\delta$  6.35, *s*) and OH-24 ( $\delta$  9.96, *s*) indicating that com-

Table 1

$^1H$  NMR spectroscopic data (500 MHz,  $CDCl_3$  for kermadecins A and B (1–2), 600 MHz for kermadecins C, D, E and F (3–6), and in  $CD_3OD$ , 600 MHz for kermadecin G and H (7–8))

|          | 1                            | 2                            | 3                            | 4                            | 5                            | 6                            | 7                            | 8                            |
|----------|------------------------------|------------------------------|------------------------------|------------------------------|------------------------------|------------------------------|------------------------------|------------------------------|
| Position | $\delta_H$ ( <i>J</i> in Hz) | $\delta_H$ ( <i>J</i> in Hz) | $\delta_H$ ( <i>J</i> in Hz) | $\delta_H$ ( <i>J</i> in Hz) | $\delta_H$ ( <i>J</i> in Hz) | $\delta_H$ ( <i>J</i> in Hz) | $\delta_H$ ( <i>J</i> in Hz) | $\delta_H$ ( <i>J</i> in Hz) |
| 1        | 2.20, <i>m</i>               | 2.23, <i>m</i>               | 2.32, <i>m</i>               | 2.30, <i>m</i>               | 2.21, <i>m</i>               | 2.21                         | 2.26, <i>m</i>               | 2.25, <i>m</i>               |
| 2        | 1.33, <i>m</i>               | 1.32, <i>m</i>               | 1.34, <i>m</i>               | 1.45, <i>m</i>               | 1.35, <i>m</i>               | 1.42, <i>m</i>               | 1.38, <i>m</i>               | 1.30, <i>m</i>               |
| 3        | 1.10, <i>m</i>               | 1.09, <i>m</i>               | 1.13, <i>m</i>               | 1.21, <i>m</i>               | 1.11, <i>m</i>               | –                            | 1.14, <i>m</i>               | 1.88, <i>m</i>               |
| 4        | –                            | –                            | –                            | –                            | –                            | –                            | –                            | 5.26, <i>m</i>               |
| 5        | –                            | –                            | –                            | –                            | –                            | –                            | –                            | 5.26, <i>m</i>               |
| 6        | –                            | –                            | –                            | –                            | –                            | –                            | –                            | 1.88, <i>m</i>               |
| 4–11     | 1.3–1.4, <i>m</i>            | 1.3–1.4, <i>m</i>            | 1.3–1.4, <i>m</i>            | 1.3–1.4, <i>m</i>            | 1.3–1.4, <i>m</i>            | 1.3–1.4, <i>m</i>            | 1.3–1.4, <i>m</i>            | 1.3–1.4, <i>m</i>            |
| 12       | 1.23, <i>m</i>               | 1.23, <i>m</i>               | 1.19, <i>m</i>               | 1.30, <i>m</i>               | 1.24, <i>m</i>               | –                            | 1.30, <i>m</i>               | 1.26, <i>m</i>               |
| 13       | 1.61, <i>q</i> (6.7)         | 1.59, <i>m</i>               | 1.58, <i>q</i> (6.8)         | 1.57, <i>q</i> (7.2)         | 1.62, <i>m</i>               | 1.63, <i>m</i>               | 1.63, <i>m</i>               | 1.65, <i>m</i>               |
| 14       | 2.56, <i>t</i> (6.7)         | 2.56, <i>t</i> (6.7)         | 2.53, <i>t</i> (6.8)         | 2.5, <i>t</i> (7.2)          | 2.57, <i>t</i> (6.6)         | 2.87–2.25                    | 2.54, <i>t</i> (6.6)         | 2.56, <i>t</i> (6.3)         |
| 16       | 6.45, <i>s</i>               | 6.39, <i>s</i>               | 6.34, <i>s</i>               | 6.46, <i>t</i> (2.1)         | 6.46, <i>s</i>               | 6.60, <i>s</i>               | 6.30, <i>s</i>               | 6.30, <i>s</i>               |
| 18       | –                            | –                            | –                            | 6.00, <i>t</i> (2.1)         | –                            | –                            | –                            | –                            |
| 20       | 6.45, <i>s</i>               | 6.39, <i>s</i>               | 6.34, <i>s</i>               | 6.30, <i>t</i> (2.1)         | 6.46, <i>s</i>               | –                            | 6.30, <i>s</i>               | 6.30, <i>s</i>               |
| 23       | –                            | –                            | –                            | –                            | –                            | –                            | –                            | 6.26, <i>d</i> (2.4)         |
| 25       | 6.44, <i>s</i>               | 6.35, <i>s</i>               | –                            | 6.25, <i>s</i>               | 6.47, <i>s</i>               | 6.24, <i>s</i>               | 6.29, <i>s</i>               | 6.33, <i>d</i> (2.4)         |
| 27       | 6.62, <i>d</i> (10.0)        | 6.59, <i>d</i> (9.9)         | 6.48, <i>d</i> (9.9)         | 6.61, <i>d</i> (9.9)         | 3.42, <i>m</i>               | 6.56, <i>d</i> (10.4)        | 4.74, <i>d</i> (7.4)         | –                            |
| 28       | 5.55, <i>d</i> (10.0)        | 5.56, <i>d</i> (9.9)         | 5.61, <i>d</i> (9.9)         | 5.55, <i>d</i> (9.9)         | 5.29, <i>m</i>               | 5.49, <i>d</i> (10.4)        | 3.65, <i>d</i> (7.4)         | –                            |
| 30       | 1.45, <i>s</i>               | 1.30, <i>s</i>               | 1.52, <i>s</i>               | 1.43, <i>s</i>               | 1.79, <i>s</i>               | 1.33, <i>s</i>               | 1.43, <i>s</i>               | –                            |
| 31       | 1.45, <i>s</i>               | 1.30, <i>s</i>               | 1.52, <i>s</i>               | 1.43, <i>s</i>               | 1.76, <i>s</i>               | 1.30, <i>s</i>               | 1.25, <i>s</i>               | –                            |
| OH-17    | 4.74, <i>s</i>               | 8.95, <i>s</i> <sup>a</sup>  | 4.70, <i>s</i>               | –                            | –                            | –                            | –                            | –                            |
| OH-19    | 4.74, <i>s</i>               | 8.95, <i>s</i> <sup>a</sup>  | 4.70, <i>s</i>               | 5.07, <i>s</i>               | –                            | 11.40, <i>s</i> <sup>a</sup> | –                            | –                            |
| OH-22    | 4.98, <i>s</i>               | –                            | –                            | 5.34, <i>s</i>               | –                            | –                            | –                            | –                            |
| OH-24    | –                            | 9.96, <i>s</i> <sup>a</sup>  | –                            | –                            | –                            | 10.27, <i>s</i> <sup>a</sup> | –                            | –                            |

<sup>a</sup> Chemical shifts obtained in DMF at 233 K on 600 MHz.

Table 2

$^{13}\text{C}$  NMR spectroscopic data (75 MHz,  $\text{CDCl}_3$  for kermadecins A and B (1–2), 150 MHz for kermadecins C, D, E and F (3–6), and in  $\text{CD}_3\text{OD}$ , 150 MHz for kermadecins G and H (7–8))

| Position | 1               | 2               | 3               | 4               | 5               | 6 <sup>a</sup>  | 7               | 8               |
|----------|-----------------|-----------------|-----------------|-----------------|-----------------|-----------------|-----------------|-----------------|
| 1        | 33.7, <i>t</i>  | 33.6, <i>t</i>  | 28.2, <i>t</i>  | 29.8, <i>t</i>  | 33.4, <i>t</i>  | 34.2, <i>t</i>  | 35.0, <i>t</i>  | 35.2, <i>t</i>  |
| 2        | 31.2, <i>t</i>  | 31.4, <i>t</i>  | 28.8, <i>t</i>  | 30.0, <i>t</i>  | 31.6, <i>t</i>  | 31.3, <i>t</i>  | 32.2, <i>t</i>  | 32.9, <i>t</i>  |
| 3        | 30.2, <i>t</i>  | 29.2, <i>t</i>  | 27.0, <i>t</i>  | 27.1, <i>t</i>  | 28.2, <i>t</i>  | 29–31, <i>t</i> | 30.1, <i>t</i>  | 29.0, <i>t</i>  |
| 4        | –               | –               | –               | –               | –               | –               | –               | 130.9, <i>d</i> |
| 5        | –               | –               | –               | –               | –               | –               | –               | 131.1, <i>d</i> |
| 6        | –               | –               | –               | –               | –               | –               | –               | 27.1, <i>t</i>  |
| 4–11     | 29–31, <i>t</i> | 29–31, <i>t</i> | 29–31, <i>t</i> | 29–31, <i>t</i> | 29–31, <i>t</i> | 29–31, <i>t</i> | 29–31, <i>t</i> | 28–30, <i>t</i> |
| 12       | 26.8, <i>t</i>  | 27.1, <i>t</i>  | 27.5, <i>t</i>  | 27.5, <i>t</i>  | 29.1, <i>t</i>  | 29–31, <i>t</i> | 28.5, <i>t</i>  | 28.0, <i>t</i>  |
| 13       | 30.2, <i>t</i>  | 30.5, <i>t</i>  | 30.1, <i>t</i>  | 30.4, <i>t</i>  | 30.3, <i>t</i>  | 27.6, <i>t</i>  | 31.6, <i>t</i>  | 31.6, <i>t</i>  |
| 14       | 35.6, <i>t</i>  | 35.7, <i>t</i>  | 35.3, <i>t</i>  | 35.6, <i>t</i>  | 35.6, <i>t</i>  | 28.0, <i>t</i>  | 36.5, <i>t</i>  | 36.7, <i>t</i>  |
| 15       | 146.8, <i>s</i> | 144.5, <i>s</i> | 146.0, <i>s</i> | 146.3, <i>s</i> | 146.7, <i>s</i> | 145.0, <i>s</i> | 145.0, <i>s</i> | 144.8, <i>s</i> |
| 16       | 108.1, <i>d</i> | 107.5, <i>d</i> | 109.0, <i>d</i> | 108.5, <i>d</i> | 108.0, <i>d</i> | 135.7, <i>d</i> | 108.4, <i>d</i> | 108.7, <i>d</i> |
| 17       | 154.5, <i>s</i> | 153.6, <i>s</i> | 153.3, <i>s</i> | 159.1, <i>s</i> | 154.4, <i>s</i> | 186.6, <i>s</i> | 157.2, <i>s</i> | 157.4, <i>s</i> |
| 18       | 103.4, <i>s</i> | 107.3, <i>s</i> | 106.4, <i>s</i> | 98.9, <i>d</i>  | 104.0, <i>s</i> | 117.5, <i>s</i> | 109.0, <i>s</i> | 109.7, <i>s</i> |
| 19       | 154.5, <i>s</i> | 153.6, <i>s</i> | 153.3, <i>s</i> | 156.7, <i>s</i> | 154.4, <i>s</i> | 152.1, <i>s</i> | 157.2, <i>s</i> | 157.4, <i>s</i> |
| 20       | 108.1, <i>d</i> | 107.5, <i>d</i> | 109.0, <i>d</i> | 109.6, <i>d</i> | 108.0, <i>d</i> | 184.1, <i>s</i> | 108.4, <i>d</i> | 108.7, <i>d</i> |
| 21       | 105.1, <i>s</i> | 108.6, <i>s</i> | 136.1, <i>s</i> | 132.9, <i>s</i> | 105.3, <i>s</i> | 110.4, <i>s</i> | 113.7, <i>s</i> | 112.6, <i>s</i> |
| 22       | 150.7, <i>s</i> | 153.3, <i>s</i> | 183.6, <i>s</i> | 144.3, <i>s</i> | 153.7, <i>s</i> | 151.6, <i>s</i> | 156.1, <i>s</i> | 157.7, <i>s</i> |
| 23       | 107.5, <i>s</i> | 108.1, <i>s</i> | 115.6, <i>s</i> | 107.8, <i>s</i> | 111.7, <i>s</i> | 107.6, <i>s</i> | 108.6, <i>s</i> | 101.6, <i>d</i> |
| 24       | 155.3, <i>s</i> | 152.2, <i>s</i> | 150.4, <i>s</i> | 150.3, <i>s</i> | 157.1, <i>s</i> | 151.9, <i>s</i> | 154.0, <i>s</i> | 159.1, <i>s</i> |
| 25       | 110.4, <i>d</i> | 109.4, <i>d</i> | 181.7, <i>s</i> | 108.7, <i>d</i> | 109.8, <i>d</i> | 108.4, <i>d</i> | 109.9, <i>d</i> | 108.9, <i>d</i> |
| 26       | 146.2, <i>s</i> | 146.7, <i>s</i> | 148.0, <i>s</i> | 136.6, <i>s</i> | 144.3, <i>s</i> | 143.8, <i>s</i> | 146.8, <i>s</i> | 147.1, <i>s</i> |
| 27       | 116.5, <i>d</i> | 116.0, <i>d</i> | 115.2, <i>d</i> | 116.6, <i>d</i> | 22.9, <i>t</i>  | 116.5, <i>d</i> | 69.9, <i>d</i>  |                 |
| 28       | 128.5, <i>d</i> | 129.1, <i>d</i> | 129.8, <i>d</i> | 128.6, <i>d</i> | 121.4, <i>d</i> | 128.7, <i>d</i> | 76.8, <i>d</i>  |                 |
| 29       | 76.6, <i>s</i>  | 76.7, <i>s</i>  | 80.5, <i>s</i>  | 76.0, <i>s</i>  | 135.2, <i>s</i> | 76.6, <i>s</i>  | 79.3, <i>s</i>  |                 |
| 30       | 28.3, <i>s</i>  | 27.6, <i>s</i>  | 28.6, <i>s</i>  | 27.9, <i>s</i>  | 17.9, <i>s</i>  | 27.5, <i>s</i>  | 26.7, <i>s</i>  |                 |
| 31       | 28.3, <i>s</i>  | 27.6, <i>s</i>  | 28.6, <i>s</i>  | 27.9, <i>s</i>  | 25.8, <i>s</i>  | 27.9, <i>s</i>  | 20.1, <i>s</i>  |                 |

<sup>a</sup> Chemical shifts obtained in  $\text{CDCl}_3$  using a time delay of 4 s.

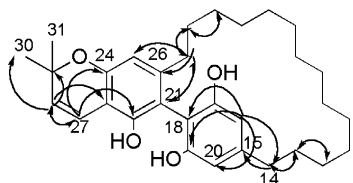


Fig. 4. Selected HMBC (single arrow) and COSY (double arrow) correlations for **1**.

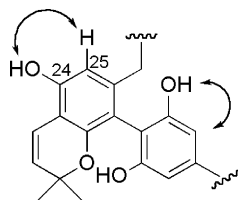


Fig. 5. Key NOESY correlations for **2**.

Compound **2** possesses the structure depicted in Fig. 5. Compound **2** was named kermadecin B.

Compound **3** has a molecular formula of  $\text{C}_{31}\text{H}_{40}\text{O}_5$  as determined by HRESIMS  $m/z$   $[\text{M} + \text{Na}]^+$  515.2784 (calcd. 515.2773). The signals of the  $^1\text{H}$  and  $^{13}\text{C}$  NMR spectra suggested that compounds **1** and **3** are closely related (Tables 1 and 2). They differed mainly by the absence of a proton signal at  $\delta$  6.44 ppm for H-25, and the presence of carbon sig-

nals at  $\delta$  181.7 and 183.6 ppm for two ketones at C-25 and C-22 in the NMR spectra of **3**, instead of signals for an hydroxy group at C-22 and a CH at C-25 in compound **1**. The paraquinone moiety fused to a dimethylpyran ring instead of a phenolic ring is also suggested by the presence of a strong band at  $1624\text{ cm}^{-1}$  in the IR spectrum of **3**. The shift of C-21 in the down field region confirmed that this carbon is located in position ortho to the quinone. The location of the dimethylpyran ring was determined by the HMBC experiment. HMBC correlations from H-27 to C-22 and H-1 to C-21 and C-26 indicated the orientation of the dimethylpyran ring as shown in **3**. These data, together with other results of COSY and HMBC analysis, confirmed that the structure of kermadecin C is **3**.

The HRESIMS of compound **4** revealed an ion peak at  $m/z$  501.3012  $[\text{M} + \text{Na}]^+$  (calcd. 501.2981) giving the molecular formula  $\text{C}_{31}\text{H}_{42}\text{O}_4$ . In contrast to compounds **1** and **2**, compound **4** showed a different proton signal pattern in the aromatic part of the  $^1\text{H}$  NMR spectrum. In addition to one proton singlet at  $\delta$  6.25 (1H, *s*, H-25), the presence of three triplet aromatic protons at  $\delta$  6.00 ppm (1H, *t*,  $J = 2.1\text{ Hz}$ , H-18), 6.30 ppm (1H, *t*,  $J = 2.1\text{ Hz}$ , H-20) and 6.46 ppm (1H, *t*,  $J = 2.1\text{ Hz}$ , H-16), suggested a 1,3,5-substituted asymmetrical aromatic ring along with the pentasubstituted aromatic ring. Long-range correlations from H-25 to C-1, H-1 to C-21 and C-25 and H-16 and H-20 to C-14 in the HMBC spectrum confirmed the

location of the carbon chain between the two aromatic rings. On the other hand, HMBC correlations were observed between H-27 and C-22, C-23 and C-24, indicating the position of the dimethylpyran ring. The shift of C-21 at  $\delta$  132.9 in the down field region suggested that this carbon is bound to an oxygen atom (Ahmed et al., 2000). As for compound **1**, no NOE interaction was observed between the hydroxy proton singlet ( $\delta$  5.34, *s*, OH-22) and the aromatic proton H-25 ( $\delta$  6.25, *s*) and between any methylene of the macrocycle and hydroxy group. These results together with those obtained from COSY and HMBC analysis suggested that the two aromatic rings are connected by an ether linkage between C-17 and C-21. Compound **4**, named kermadecin D, is an analogue of greviobstol B isolated from *Grevillea robusta* (Ahmed et al., 2000).

Compound **5** showed in its HRESIMS a molecular ion  $[M-H]^-$  at  $m/z$  479.3147, compatible with a molecular formula  $C_{31}H_{44}O_4$  (calcd. 479.3161), which suggested the presence of two additional protons. In the LC/APCI-MS analysis, in negative-ion mode, it has been observed that a fragment of 110 amu was lost from the quasi molecular peak at  $m/z$  477, suggesting that compound **5** possesses a prenyl substituent. This prenyl unit is confirmed by the observation of signals at  $\delta$  3.42 (2H, *m*, H-22), 5.29 (1H, *m*, H-28) 1.76 (3H, *s*, H-31) and 1.79 (3H, *s*, H-30) in the  $^1H$  NMR spectrum. The location of the substituents were elucidated by HMBC analysis. The location of the prenyl group at C-23 and the aliphatic chain between the two aromatic rings at C-15 and C-26 were confirmed by observation of C–H long range correlations from H-27 to C-22 and C-24, H-1 to C-21, H-25 to C-1, C-21, C-23 and C-25 and H-16 and H-20 to C-14. Thus the structure **5** was established for kermadecin E.

The HRESIMS of compound **6** indicated an ion peak  $m/z$  515.2798  $[M+Na]^+$  (calcd. 515.2773) giving the molecular formula  $C_{31}H_{40}O_5$ . The IR spectrum of **6** showed absorption bands at  $3238\text{ cm}^{-1}$  for hydroxy groups,  $1608$  and  $1423\text{ cm}^{-1}$  for an aromatic ring and a strong band at  $1632\text{ cm}^{-1}$  suggesting a paraquinone moiety, confirmed in the  $^{13}C$  NMR spectrum by the presence of signals at 186.6 and 184.1 ppm for two ketones at C-17 and C-20, respectively. The presence of a dimethylpyran ring fused to a phenol ring has been confirmed with MS fragmentation analysis and  $^1H$  and  $^{13}C$  NMR data (Tables 1 and 2). In the HMBC spectrum, correlations from H-16 to C-14, C-18 and C-20 and from H-14 to C-16 and C-20 suggested that the trisubstituted paraquinone was located as shown in structure **6**. Other HMBC correlations were similar to those observed for compound **2**, indicating that the dimethylpyran ring is fused to the aromatic ring in a similar way to **2**. This was confirmed by the correlation between H-25 ( $\delta$  6.24, *s*) and OH-24 ( $\delta$  10.27, *s*) observed in the NOESY spectrum, obtained in DMF at a temperature of 233 K. Moreover, in contrast to compound **2**, no NOE correlation between the aromatic singlet H-16 ( $\delta$  6.60, *s*) and the hydroxy proton at  $\delta_H$  11.40 was observed,

indicating the location of the hydroxy group on carbon C-19. These data confirmed that the structure of kermadecin F is **6**. In contrast to compounds **1–3** and **5**, kermadecin F possesses a chiral biaryl axis arising from the presence of the asymmetric paraquinone moiety. Consequently, compound **6** showed optical activity ( $[\alpha]_D^{25} - 16^\circ$ ).

The HRESIMS of compound **7** revealed an ion peak at  $m/z$  535.3107  $[M+Na]^+$  (calcd. 535.3036) corresponding to the molecular formula  $C_{31}H_{44}O_6$ . Thus the molecule showed two additional hydroxy groups when compared with **1**. In the  $^1H$  NMR spectrum, the two vinylic protons are replaced by two coupled protons at  $\delta$  3.65 (1H, *d*,  $J = 7.4$ , H-28) and 4.74 (1H, *d*,  $J = 7.4$ , H-27). The characteristic chemical shifts and coupling constants of these protons indicated the presence of a 3,4-*trans*-dihydroxy-2,2-dimethylchroman moiety (Morel et al., 2002). HMBC correlations were observed between H-25 and C-1, C-21 and C-23, H-28 and C-27, C-29, C-30 and C-31, and H-27 and C-22, C-23, C-24 and C-28, indicating that the phenyl ring was substituted with the 3,4-*trans*-dihydroxy-2,2-dimethylchroman moiety at C-23, C-24 as shown in **7**. Compound **7** was isolated as a racemic mixture since no optical rotation could be measured and HPLC on a chiral column showed two peaks with a ratio of 50:50. These data, together with other results of HMBC analysis suggested that this mixture of enantiomers, named kermadecin G possesses structure **7**.

Compound **8** gave a HRESIMS spectrum with an ion peak at  $m/z$   $[M+Na]^+$  433.2426 (calcd. 433.2355) compatible with the molecular formula  $C_{26}H_{34}O_4$ . In comparison to **5**, the loss of  $C_5H_{10}$  suggested the loss of an isoprenyl group and the presence of an additional double bond in the chain. This is confirmed in the LC/APCI-MS study where neither the ion at  $m/z$  367 nor the ion at  $m/z$  107 were observed in negative-ion mode. On the other hand, in positive-ion mode, the presence of the ion at  $m/z = 297$ , resulting from the loss of a fragment of 180 amu, suggested the presence of a mono-unsaturated long carbon chain. In the aromatic part of the  $^1H$  NMR spectrum, four aromatic protons appearing as two proton doublets at  $\delta$  6.26 (1H, *d*,  $J = 2.4$ , H-23) and 6.33 (1H, *d*,  $J = 2.4$ , H-25) and two-protons singlet at  $\delta$  6.30 (2H, *s*, H-20) suggested a 1,2,3,5-tetrasubstituted and a symmetrical tetrasubstituted aromatic rings, respectively. The presence of a multiplet signal at  $\delta$  5.26 (2H, *m*, H-4 and H-5) in the  $^1H$  NMR spectrum and signals at  $\delta$  130.9 and 131.1 (C-4 and C-5, respectively) in the  $^{13}C$  NMR spectrum were compatible with an additional double bond in the chain. In the  $^1H$ - $^1H$  COSY spectrum, the observation of correlations between protons at  $\delta$  1.88 (2H, *m*, H-3) and at  $\delta$  1.30 (2H, *m*, H-2) and 5.26 (2H, *m*, H-4 and H-5), and between protons at  $\delta$  1.30 (2H, *m*, H-2) and 2.25 (2H, *m*, H-1), suggested that the protons at  $\delta$  2.25, 1.30, 1.88 and 5.26 were assigned to  $CH_2$ -1,  $CH_2$ -2,  $CH_2$ -3, CH-4 and CH-5, respectively, indicating the position of the double bond between C-4 and C-5. The presence of allylic carbon resonances at  $\delta$  29.0 and 27.1, C-3 and



Table 3  
*In vitro* cytotoxic activity of compounds **1–4** (IC<sub>50</sub> in  $\mu$ M)

|                 | 1   | 2   | 3    | 4    | Taxotere |
|-----------------|-----|-----|------|------|----------|
| L1210 cell line | 6.3 | 4.1 | 18.5 | 15.0 | 0.004    |
| KB cell line    | 3.6 | 4.4 | >10  | >10  | 0.00016  |

C-6, respectively, and olefinic carbon resonances at  $\delta$  130.9 and 131.1, C-4 and C-5, allowed to propose the configuration *Z* for the geometry of the double bond (Rossi et al., 1982). Other COSY and HMBC correlations were identical with that of compound **1** and allowed to propose the structure **8** for kermadecin H. This compound is closely related to the one found in *Grevillea striata* (Ridley et al., 1970).

Compounds **1–4** were subjected to a cytotoxic assay against KB and L1210 cancer cell lines (Table 3). Kermadecins A and B showed a significant activity against L1210 and KB cells, with IC<sub>50</sub> values within the micromolar range, whereas kermadecins C and D had weak cytotoxic activities.

### 3. Conclusions

The study of *Kermadecia elliptica* has led to the isolation of eight new molecules: kermadecins A–H (**1–8**). This is the first report of secondary metabolites isolated from the genus *Kermadecia*. Their isolation is a consequence of a random screening of New Caledonian plant extracts in a cytotoxic assay, and the use of a LC/MS method to detect and to direct purification of this series of molecules.

### 4. Experimental

#### 4.1. General experimental procedures

IR spectra were obtained on a Nicolet FTIR 205 spectrophotometer and UV spectra on a Perkin–Elmer Lambda 5 spectrophotometer. The NMR spectra were recorded on a Bruker spectrometer 500 MHz for <sup>1</sup>H and 150 MHz for <sup>13</sup>C (compounds **1–3**) and on a Bruker Avance 600 MHz for <sup>1</sup>H and 150 MHz for <sup>13</sup>C (compounds **4–8**) using CDCl<sub>3</sub> (compounds **1–6**), MeOD (compounds **7–8**) and DMF-d<sub>6</sub> (compounds **2,6**) as solvent. A time delay of 4 s was used for the <sup>13</sup>C NMR spectrum of compound **6** (12288 scans). Chemical shifts (relative to TMS) are in ppm, and coupling constants (in brackets) in Hz. ESIMS was obtained on a Navigator mass Thermoquest. HRESIMS were obtained on a MALDI-TOF spectrometer (Voyager-De STR; Perseptive Biosystems). The HPLC separations were performed using a Waters autopurification equipped with a UV–Vis diode array detector (190–600 nm) and a PI-ELS 1000 ELSD detector Polymer laboratory. Reversed-phase Kromasil C-18 column (250 × 21.2 mm I.D., 5  $\mu$ m) were used for preparative chromatography. LC-APCIMS analyses were performed using

Finnigan Surveyor HPLC system and ion trap MSn (Finnigan LCQDeca) detector. Kromasil C-18 column (210 × mm I.D., 5  $\mu$ m) was used for analytical analysis. A gradient mobile phase consisting of acetonitrile/water 20:80 to 100:0 at 0.7 ml/min in 75 min was used to analyse fractions.

The Finnigan detector was equipped with an atmospheric pressure chemical ionisation (APCI) source operating under the following conditions: sheath gas flow rate: 80 (arbitrary units), N<sub>2</sub>, capillary temperature: 250 °C, discharge current: 4.5  $\mu$ A, vaporizer temperature: 450 °C, capillary voltage: 15 V.

Full scan mass spectra (50–800 amu) were recorded alternatively in positive and negative mode. For MS<sup>2</sup>, the data dependent program was used so that the most abundant ions in each scan were selected and subject to MS<sup>2</sup> analyses. The collision-induced dissociation (CID) energy was adjusted to 50%. The isolation width of precursor ion was 2.0 mass units.

#### 4.2. Plant material

The bark of *Kermadecia elliptica* Brongniart & Gris (Proteaceae) was collected in 2004 at “Forêt plate”. The collection was made by one of us (V.D.) in a dense rain forest, 15 km East to the special reserve of fauna of Aoupinié, Northern Province, New Caledonia (21°8'20,515" S; 165°6'47,492" E, elevation 460 m). The specimen accessed was a medium tree 18 m in height, with leathery elliptical leaves, rubiginous then shiny above, and light brown axillary inflorescence on branches. The corresponding voucher specimen DUM-0459 is kept at the Herbarium of the Botanical and Tropical Ecology Department of the IRD Center, Nouméa, New Caledonia.

#### 4.3. Extraction and isolation

Air-dried material (3 kg) was extracted with EtOAc (3 × 4.5 l, 1 h each) at room temperature and concentrated under vacuum at 40 °C. The EtOAc extract (17 g) was submitted to a silica gel column chromatography using a gradient of *n*-hexane-CH<sub>2</sub>Cl<sub>2</sub> (80:20–0:100) and CH<sub>2</sub>Cl<sub>2</sub>-MeOH (100:0–80:20) to give 18 fractions (fractions 1–18) according to their TLC profile.

Fraction 9 was submitted to a flash chromatography on reversed-phase (VersaPack, C-18 Cartridge 40 × 75 mm) using a gradient mobile phase consisting of H<sub>2</sub>O-MeCN 50:50–0:100 at 10 ml/min, to give 9 fractions (fractions 9–1 to 9–9, 100 ml each). Fraction 9–6 was finally submitted to HPLC purification on a semi-preparative Symmetry Shield RP18 column (250 × 10 mm, 7  $\mu$ m). An isocratic mobile phase MeCN-H<sub>2</sub>O 70:30 at a flow rate of 7.9 ml min<sup>−1</sup> afforded kermadecin A (**1**) (t<sub>R</sub> 25 min, 40 mg). The same method was applied to fraction 10. Preparative HPLC purification performed on fraction 10–7 (C-18 Kromasil column, 250 × 21.2 mm, I.D., 5  $\mu$ m) using a mobile phase consisting of MeCN-H<sub>2</sub>O 75:35 during

60 min and 100:0 during 20 min at a flow rate of  $21.2 \text{ ml min}^{-1}$  afforded kermadecin A (**1**) ( $t_R$  45 min, 63 mg) and kermadecin D (**4**) ( $t_R$  70 min, 8 mg). From fraction 10–5, a semi-preparative C-18 Kromasil column, (250  $\times$  10 mm, I.D., 5  $\mu\text{m}$ ) using an isocratic mobile phase consisting of MeCN–H<sub>2</sub>O 60:40 at  $4.7 \text{ ml min}^{-1}$  was used to purify kermadecin E (**5**) ( $t_R$  64 min, 1 mg).

Fraction 11 was submitted to a flash chromatography on reversed-phase in the same conditions than fractions 9 and 10. Fraction 11–6 was finally submitted to a preparative HPLC using an isocratic mobile phase MeCN–H<sub>2</sub>O 65:35 at a flow rate of  $21.2 \text{ ml min}^{-1}$  to give kermadecin B (**2**) ( $t_R$  75 min, 26 mg) and kermadecin C (**3**) ( $t_R$  54 min, 3.2 mg).

Fraction 5 was submitted to a flash chromatography on reversed-phase (VersaPack, C18 Cartridge 40  $\times$  75 mm) using a gradient mobile phase consisting of MeCN–H<sub>2</sub>O 50:50–0:100 at 10 ml/min to give 7 fractions (fractions 5–1 to 5–7). Fraction 5–5 was submitted to reverse HPLC on a semipreparative C-18 Kromasil column with a gradient mobile phase consisting of MeCN–H<sub>2</sub>O 20:80 (5 min), 20:80 (15 min), 0:100 (45 min) at  $4.7 \text{ ml min}^{-1}$  to give Kermadecin F (**6**) ( $t_R$  29 min, 8 mg).

Fraction 13 was submitted to a semi-preparative HPLC using an isocratic mobile phase consisting of MeCN–H<sub>2</sub>O 70:30 at a flow rate of  $4.7 \text{ ml min}^{-1}$ , afforded two fractions (fractions 13–1, 11–15 min and 13–2, 25–27 min). From fraction 13-2, a semipreparative HPLC using an isocratic mobile phase MeCN–H<sub>2</sub>O 70:30 at a flow rate of  $4.7 \text{ mL min}^{-1}$  afforded kermadecin G (**7**) ( $t_R$  30 min, 2.3 mg) and from fraction 13–1 an isocratic mobile phase consisting of MeCN–H<sub>2</sub>O 55:45 afforded kermadecin H (**8**) ( $t_R$  32 min, 2 mg). Kermadecin G was subjected to an analytical HPLC (chiral column Chiralcel OD, 250  $\times$  4.6 mm, 10  $\mu\text{m}$ , mobile phase: Hexane – EtOH 85:15 at a flow rate of  $1 \text{ ml min}^{-1}$ ) and showed the presence of a racemic mixture ( $t_R$ : 7.6 and 9.0 min).

#### 4.4. Kermadecin A (**1**)

Purple amorphous solid; UV (MeOH)  $\lambda_{\text{max}}$  (log  $\epsilon$ ), 204 nm (4.63), 231 nm (4.60), 280 nm (4.15); IR  $\nu_{\text{max}}$  3518, 2900, 1616 and  $1426 \text{ cm}^{-1}$ ;  $^1\text{H}$  NMR (CDCl<sub>3</sub>, 500 MHz) see Table 1;  $^{13}\text{C}$  NMR (CDCl<sub>3</sub>, 150 MHz), see Table 2; EIMS  $m/z$  501.2 [M + Na]<sup>+</sup>, 479.3 [M + H]<sup>+</sup>; HRESIMS  $m/z$  [M + Na]<sup>+</sup> 501.3071 (calcd. for C<sub>31</sub>H<sub>42</sub>O<sub>4</sub>Na, 501.2981).

#### 4.5. Kermadecin B (**2**)

Orange amorphous solid; UV (MeOH)  $\lambda_{\text{max}}$  (log  $\epsilon$ ), 201 nm (4.33), 204 nm (4.33), 226 (4.21) and 282 (3.73); IR  $\nu_{\text{max}}$  3410, 2900, 1573 and  $1419 \text{ cm}^{-1}$ ;  $^1\text{H}$  NMR (CDCl<sub>3</sub>, 500 MHz), see Table 1;  $^{13}\text{C}$  NMR (CDCl<sub>3</sub>, 150 MHz), see Table 2; EIMS  $m/z$  501.4 [M + Na]<sup>+</sup>; HRESIMS  $m/z$  [M + Na]<sup>+</sup> 501.3072 (calcd. for C<sub>31</sub>H<sub>42</sub>O<sub>4</sub>Na, 501.2981).

#### 4.6. Kermadecin C (**3**)

Red amorphous solid; UV (MeOH)  $\lambda_{\text{max}}$  (log  $\epsilon$ ), 204 nm (4.55), 276 (3.99); IR  $\nu_{\text{max}}$  3389, 2926, 2361, 2338 and  $1624 \text{ cm}^{-1}$ ;  $^1\text{H}$  NMR (CDCl<sub>3</sub>, 600 MHz), see Table 1;  $^{13}\text{C}$  NMR (CDCl<sub>3</sub>, 150 MHz), see Table 2; EIMS  $m/z$  515.3 [M + Na]<sup>+</sup>, 441.3, 376.2, 243.2; HRESIMS  $m/z$  [M + Na]<sup>+</sup> 515.2784 (calcd. for C<sub>31</sub>H<sub>40</sub>O<sub>5</sub>Na, 515.2773).

#### 4.7. Kermadecin D (**4**)

Brown amorphous solid, UV (MeOH)  $\lambda_{\text{max}}$  (log  $\epsilon$ ), 203 nm (4.55), 230 nm (4.34), 277 nm (3.95); IR  $\nu_{\text{max}}$  3408, 2924, 2853, 1591 and  $1439 \text{ cm}^{-1}$ ;  $^1\text{H}$  NMR (CDCl<sub>3</sub>, 600 MHz), see Table 1;  $^{13}\text{C}$  NMR (CDCl<sub>3</sub>, 150 MHz), see Table 2; EIMS  $m/z$  501.3 [M + Na]<sup>+</sup>, 479.3, [M + H]<sup>+</sup>, 463.3, 429.3, 413.3; HRESIMS  $m/z$  [M + Na]<sup>+</sup> 501.3012 (calcd. for C<sub>31</sub>H<sub>42</sub>O<sub>4</sub>Na, 501.2981).

#### 4.8. Kermadecin E (**5**)

Purple amorphous solid, UV (MeOH)  $\lambda_{\text{max}}$  210 nm, 280 nm; IR  $\nu_{\text{max}}$  3400 and  $1700 \text{ cm}^{-1}$ ;  $^1\text{H}$  NMR (CDCl<sub>3</sub>, 600 MHz), see Table 1;  $^{13}\text{C}$  NMR (CDCl<sub>3</sub>, 150 MHz), see Table 2; EIMS  $m/z$  479.3 [M–H]<sup>–</sup>, 481.3 [M + H]<sup>+</sup>; HRESIMS  $m/z$  [M–H]<sup>–</sup> 479.3147 (calcd. for C<sub>31</sub>H<sub>43</sub>O<sub>4</sub>, 479.3161).

#### 4.9. Kermadecin F (**6**)

Red amorphous solid;  $[\alpha]_D^{25} - 16^\circ$  ( $c$  0.1, CH<sub>2</sub>Cl<sub>2</sub>). UV (MeOH)  $\lambda_{\text{max}}$  (log  $\epsilon$ ), 202.0 nm (8.49) and 277 nm (7.5); IR  $\nu_{\text{max}}$  3238, 2923, 2853, 1632, 1608,  $1423 \text{ cm}^{-1}$ ;  $^1\text{H}$  NMR (CDCl<sub>3</sub>, 600 MHz), see Table 1;  $^{13}\text{C}$  NMR (CDCl<sub>3</sub>, 150 MHz), see Table 2; EIMS  $m/z$  515.3 [M + Na]<sup>+</sup>; HRESIMS  $m/z$  [M + Na]<sup>+</sup> 515.2798 (calcd. for C<sub>31</sub>H<sub>40</sub>O<sub>5</sub>Na, 515.2773).

#### 4.10. Kermadecin G (**7**)

Purple amorphous solid;  $[\alpha]_D^{25} = 0$  ( $c$  = 0.1, CHCl<sub>3</sub>); UV (MeOH)  $\lambda_{\text{max}}$  (log  $\epsilon$ ), 211 nm (4.73), 280 nm (3.78); IR  $\nu_{\text{max}}$  3384, 2923.6, 2853.2, 1725.6, 1621.7 and  $1572.6 \text{ cm}^{-1}$ ;  $^1\text{H}$  NMR (MeOD, 600 MHz), see Table 1;  $^{13}\text{C}$  NMR (MeOD, 150 MHz), see Table 2; EIMS  $m/z$  535.3 [M + Na]<sup>+</sup>, 513.3 [M + H]<sup>+</sup>, 511.9 [M–H]<sup>–</sup>; HRESIMS  $m/z$  [M + Na]<sup>+</sup> 535.3107 (calcd. for C<sub>31</sub>H<sub>44</sub>O<sub>6</sub>Na, 535.3036).

#### 4.11. Kermadecin H (**8**)

Purple amorphous solid; UV (MeOH)  $\lambda_{\text{max}}$  (log  $\epsilon$ ), 208 nm (5.04), 280 nm (4.03); IR  $\nu_{\text{max}}$  3383, 2925 and  $1587 \text{ cm}^{-1}$ ;  $^1\text{H}$  NMR (MeOD, 600 MHz), see Table 1;  $^{13}\text{C}$  NMR (MeOD, 150 MHz), see Table 2; EIMS  $m/z$  433.2 [M + Na]<sup>+</sup>; HRESIMS  $m/z$  [M + Na]<sup>+</sup> 433.2426 (calcd. for C<sub>26</sub>H<sub>34</sub>O<sub>4</sub>Na, 433.2355).

#### 4.12. Cell culture assay for cytotoxicity activity

The human KB and murine L1210 tumor cell lines were originally obtained from the American Type Culture Collection (ATCC, Rockville, MD). The cytotoxic assays were performed according to a published procedures. (Pierre et al., 1991; Tempete et al., 1995).

#### Acknowledgements

This work was supported by an ICSN-CNRS grant to one of us (C.J.). We express our thanks to G. Aubert (ICSN), who performed the cytotoxic assays on KB cells.

#### References

- Ahmed, A.S., Nakamura, N., Meselhy, M.R., Makhboul, M.A., El-Emary, N., Hattori, M., 2000. Phenolic constituents from *Grevillea robusta*. *Phytochemistry* 53, 149–154.
- Bick, I.R.C., Gillard, J.W., Leow, H., 1979. Alkaloids of *Bellendenia montana*. *Aust. J. Chem.* 32, 1827–1840.
- Butler, M.S., Katavic, P.L., Davis, R.A., Forster, P.I., Guymer, G.P., Quinn, R.J., 2000. 10-Hydroxydarlingine, a tropane alkaloid from the Australian Proteaceous plant *Triunia erythrocarpa*. *J. Nat. Prod.* 63, 688–689.
- Cannon, J.R., Chow, P.W., Fuller, M.W., Hamilton, B.H., Metcalf, B.W., Power, A.J., 1973. Phenolic constituents of *Grevillea robusta* (Proteaceae). The structure of robustol, a macrocyclic phenol. *Aust. J. Chem.* 26, 2257–2275.
- Cannon, J.R., Metcalf, B.W., 1971. Phenolic constituents of *Persoonia elliptica* (Proteaceae). *Aust. J. Chem.* 24, 1925–1931.
- Chuang, T.H., Wu, P.L., 2007. Cytotoxic 5-alkylresorcinol metabolites from the leaves of *Grevillea robusta*. *J. Nat. Prod.* 70, 319–323.
- Furstner, A., Stelzer, F., Rumbo, A., Krause, H., 2002. Total synthesis of the turrianes and evaluation of the DNA-cleaving properties. *Chemistry* 8, 1856–1871.
- Lounasmaa, M., Pusset, J., Sevenet, T., 1980. Benzyl-2 tropanes et (-) -pyranotropanes, alcaloïdes de *Knightia strobilina*. *Phytochemistry* 19, 949–952.
- Mock, J., Murphy, S.T., Ritchie, E., Taylor, W.C., 1973. Chemical studies of the Proteaceae. VI Two naphthoquinones from *Stenocarpus salignus*. *Aust. J. Chem.* 26, 1121–1130.
- Morel, C., Hay, A.-E., Litaudon, M., Sévenet, T., Séraphin, D., Bruneton, J., Richomme, P., 2002. Thirteen xanthone derivatives from *Calophyllum caledonicum* (Clusiaceae). *Molecules* 7, 38–50.
- Pierre, A., Kraus-Berthier, L., Atassi, G., Cros, S., Poupon, M.F., Lavielle, G., Berlion, M., Bizzari, J.P., 1991. Preclinical antitumor activity of a *Vinca* alkaloid derivative, S 12363. *Cancer Res.* 51, 2312–2318.
- Ridley, D.D., Ritchie, E., Taylor, W.C., 1970. Chemical studies of the Proteaceae. IV. The structures of the major phenols of *Grevillea striata*; a group of cyclophanes. *Aust. J. Chem.* 23, 147–183.
- Ritchie, E., Taylor, W.C., Vautin, S.T.K., 1965. Chemical studies of the Proteaceae. I. *Grevillea robusta* A. Cunn. and *Orites excelsa* R. Br. *Aust. J. Chem.* 18, 2015–2020.
- Rossi, R., Carpita, A., Quirici, M.G., Veracini, C.A., 1982. Insect pheromone components: Use of <sup>13</sup>C NMR spectroscopy for assigning the configuration of C=C double bonds of monoenic or dienic pheromone components and for quantitative determination of *Z/E* mixtures. *Tetrahedron* 38, 639–644.
- Tempete, C., Werner, G.H., Favre, F., Rojas, A., Langlois, N., 1995. *In vitro* cytostatic activity of 9-demethoxyprothramycin B. *Eur. J. Med. Chem.* 30, 647–650.